

Internal Transitions of Two-Dimensional Charged Magneto-Excitons X^- : Theory and Experiment

A. B. Dzyubenko*

Institut für Theoretische Physik, J.W. Goethe-Universität, 60054 Frankfurt, Germany

A. Yu. Sivachenko

The Weizmann Institute of Science, Rehovot 76100, Israel

H. A. Nickel, T. M. Yeo, G. Kioseoglou, B. D. McCombe, and A. Petrou

*Department of Physics and Center for Advanced Photonic and Electronic Materials, SUNY Buffalo, Buffalo, NY
14260, USA*

(June 15, 2021)

Internal spin-singlet and spin-triplet transitions of charged excitons X^- in magnetic fields in quantum wells have been studied experimentally and theoretically. The allowed X^- transitions are photoionizing and exhibit a characteristic double-peak structure, which reflects the rich structure of the magnetoexciton continua in higher Landau levels (LL's). We discuss a novel exact selection rule, a hidden manifestation of translational invariance, that governs transitions of charged mobile complexes in a magnetic field.

73.20.Dx, 71.70.Di, 76.40.+b, 78.90.+t

Recently there has been considerable interest in charged excitonic complexes, X^- and X^+ , commonly referred to as trions. The X^- complex, which can be observed in photoluminescence- and reflectance spectra of low-density, quasi-2D electron gases (2DEGs), has been the subject of extensive experimental and theoretical work since its observation in 1993 [1]. The bulk of this work to date has been concerned with *inter*-band transitions only. *Intra*-band, or internal, transitions of X^- , which lie in the far-infrared (FIR), can provide additional important insight into the properties of the ground and excited states of this complex.

The X^- -complex, consisting of an exciton binding an additional electron, is superficially similar to its close relative, the negatively charged donor ion, D^- [2]. Both complexes are often considered to be the semiconductor analogs of the hydrogen ion, H^- . When the H^- ion is treated in the infinite proton mass approximation, such analogy is exact for the D^- complex — a localized positive charge binding two electrons. This analogy fails, however, in certain very important aspects for the *mobile* X^- complex. In particular, we show here that the magnetic translations for the X^- imply the existence of an exact selection rule that *prohibits* certain bound-to-bound internal X^- transitions, the analogs of which are very strong for the D^- . In an arbitrary uniform B this selection rule is applicable to charged electron-hole, as well as to one-component electron systems. In the latter case Kohn's theorem [3] based

on translational invariance also works. Due to the center-of-mass separation for electron systems in B , both theorems — though based on different operator algebras — give in this case equivalent predictions. To understand the main qualitative features, we first consider the strictly-2D electron-hole ($e-h$) system in high magnetic fields. In this limit, $\hbar\omega_{ce}, \hbar\omega_{ch} \gg E_0 = \sqrt{\pi/2} e^2/\epsilon l_B$, where E_0 is the binding energy of the 2D magnetoexciton (MX) in zero LL's [4] and $l_B = (\hbar c/eB)^{1/2}$. The mixing between different LL's can then be neglected, and the X^- states can be classified by total electron and hole LL numbers, $(N_e N_h)$. The corresponding basis for X^- is of the form [5] $\phi_{n_1 m_1}^{(e)}(\mathbf{r}) \phi_{n_2 m_2}^{(e)}(\mathbf{R}) \phi_{N_h M_h}^{(h)}(\mathbf{r}_h)$, and includes different three-particle $2e-h$ states such that the total angular momentum projection $M_z = N_e - N_h - m_1 - m_2 + M_h$ (and $N_e = n_1 + n_2$, N_h) are fixed. Here $\phi_{nm}^{(e,h)}$ are the e - and h - single-particle factored wave functions in B ; n is the LL quantum number; and m is the oscillator quantum number [$m_{ze(h)} = \begin{smallmatrix} + \\ - \end{smallmatrix} (n - m)$]. We use the electron relative and center-of-mass coordinates: $\mathbf{r} = (\mathbf{r}_{e1} - \mathbf{r}_{e2})/\sqrt{2}$ and $\mathbf{R} = (\mathbf{r}_{e1} + \mathbf{r}_{e2})/\sqrt{2}$. Permutational symmetry requires that for electrons in the spin-singlet s (triplet t) state the relative motion angular momentum $n_1 - m_1$ should be even (odd). This basis complies with the axial symmetry about the z -axis and the permutational symmetry. The symmetry associated with magnetic translations (e.g., [6]) and its consequences are still hidden at this point.

The calculated three-particle $2e-h$ eigenspectra (electrons in the triplet state) in the two lowest LL's are shown in Fig. 1.

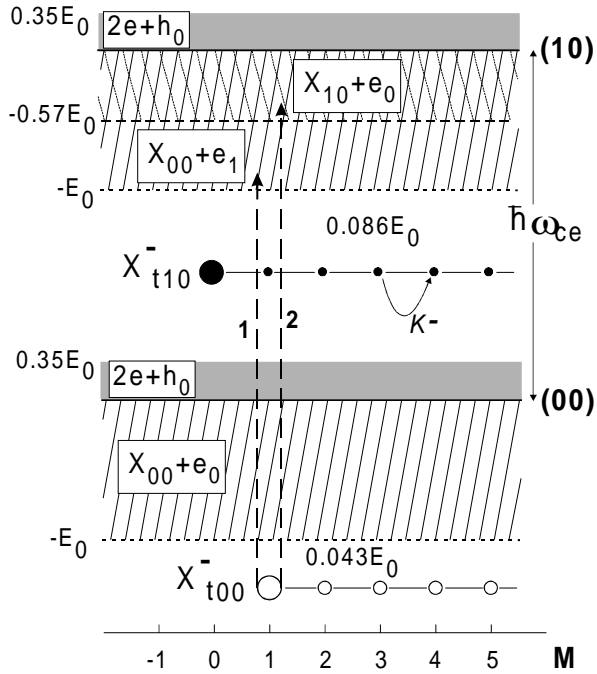


FIG. 1. Schematic drawing of bound and scattering electron triplet $2e-h$ states in the lowest LL's $(N_e N_h) = (00)$, (10) . The quantum number $M = -M_z$ for the $(N_e N_h) = (00)$ states and $M = 1 - M_z$ for the $(N_e N_h) = (10)$ states; allowed transitions must satisfy $\Delta N_e = 1$; $\Delta M_z = 1$; $\Delta k = 0$. The energy $E_0 = \sqrt{\pi/2} e^2 / \epsilon l_B$ parametrizes the 2D system in the limit of high B . Large (small) dots correspond to the bound parent (daughter) X^- states; see text for further explanations.

Generally, the eigenspectra associated with each LL consist of bands of *finite* width $\sim E_0$. The states within each such band form a *continuum* corresponding to the extended motion of a neutral magnetoexciton (MX) as a whole with the second electron in a scattering state. As an example, the continuum in the lowest $(N_e N_h) = (00)$ LL consists of the MX band of width E_0 extending down in energy from the free (00) LL. This corresponds to the $1s$ exciton ($N_e = N_h = 0$) plus a scattered electron in the zero LL, labeled $X_{00} + e_0$. The structure of the continuum in the $(N_e N_h) = (10)$ LL is more complicated: in

addition to the $X_{00} + e_1$ band of the width E_0 , there is another MX band of width $0.574E_0$ also extending down in energy from the free $(N_e N_h) = (10)$ LL. This corresponds to the $2p^+$ exciton ($N_e = 1$, $N_h = 0$) [4] plus a scattered electron in the $N_e = 0$ LL, labeled $X_{10} + e_0$. Moreover, there is a band above each free LL originating from the bound internal motion of two electrons with the hole in a scattering state (labeled $2e + h_0$) [7].

Bound X^- states (finite internal motions of all three particles) lie *outside* the continua (Fig. 1). In the limit of high B the only bound X^- state in the zeroth LL $(N_e N_h) = (00)$ is the X^- -triplet. There are no bound X^- -singlet states [8,9] in contrast to the $B = 0$ case. The X^- -triplet binding energy in zero LL's $(N_e N_h) = (00)$ is $0.043E_0$ [8,9]. In the next electron LL $(N_e N_h) = (10)$ there are no bound X^- -singlets, and only one bound triplet state X_{t10}^- , lying below the lower edge of the MX band [7]. The X_{t10}^- binding energy is $0.086E_0$, twice that of the X_{t00}^- , and similar to the stronger binding of the D^- -triplet in the $N_e = 1$ LL [5].

We focus here on internal transitions in the σ^+ polarization governed by the usual selection rules: spin conserved, $\Delta M_z = 1$. In this case the e -CR-like inter-LL ($\Delta N_e = 1$) transitions are strong and gain strength with B . Both bound-to-bound $X_{t00}^- \rightarrow X_{t10}^-$ and photoionizing X^- transitions are possible. For the latter the final three-particle states in the (10) LL belong to the continuum (Fig. 1), and calculations show that the FIR absorption spectra reflect its rich structure [7]. Transitions to the $X_{00} + e_1$ continuum are dominated by a sharp onset at the edge (transition 1) at an energy $\hbar\omega_{ce}$ plus the X_{t00}^- binding energy. In addition, there is a broader and weaker peak corresponding to the transition to the $X_{01} + e_0$ MX band, transition 2. The latter may be thought of as the $1s \rightarrow 2p^+$ internal transition of the MX [10,11], which is shifted and broadened by the presence of the second electron. Photoionizing transitions to the $2e + h_0$ band have extremely small oscillator strengths and are not considered further.

The inter-LL bound-to-bound transition, $X_{t00}^- \rightarrow X_{t10}^-$, lies *below* the e -CR energy $\hbar\omega_{ce}$. In contrast to the analogous, strong triplet T^- transition for D^- [5,12,13] this transition for X^- has exactly *zero* oscillator strength, a hidden manifestation of the magnetic translational invariance [7]. Consider the operator $\hat{\mathbf{K}} = \sum_j (\boldsymbol{\pi}_j - \frac{e_j}{c} \mathbf{r}_j \times \mathbf{B})$, which commutes with the Hamiltonian of interacting charged particles in a uniform \mathbf{B} ; here $\boldsymbol{\pi}_j = -i\hbar \nabla_j - \frac{e_j}{c} \mathbf{A}(\mathbf{r}_j)$ is the kinematic momentum of the j -th particle. The components of $\hat{\mathbf{K}} = (\hat{K}_x, \hat{K}_y)$ are the generators of magnetic translations ([6] and references therein)

and commute as canonically conjugate operators: $[\hat{K}_x, \hat{K}_y] = i\frac{\hbar B}{c} \sum_j e_j$. For the X^- , therefore, the operators $\hat{k}_\pm = (\hat{K}_x \pm i\hat{K}_y)l_B/\sqrt{2}\hbar$ are the intra-LL lowering and raising operators. Thus $(\hbar/l_B)^2\hat{\mathbf{K}}^2$ has the oscillator eigenvalues $2k+1$ ($k = 0, 1, \dots$). There is the macroscopic Landau degeneracy in the discrete quantum number k , and k can be used, together with M_z , to label the exact eigenstates. The additional selection rule is conservation of k for dipole-allowed transitions [14].

As a result of the macroscopic degeneracy of k , there exist *families* of bound, degenerate X^- states in B . One family of X^- bound states is associated with the (00) and (10) LL's. Each i -th family starts with its *Parent State* (PS) $|\Psi_{M_z}^{(P_i)}\rangle$, which has the maximal possible value of M_z in the family, (Fig. 1). The daughter states in the i -th family, $|\Psi_{M_z-l}^{(D_i)}\rangle = \hat{k}_-^l |\Psi_{M_z}^{(P_i)}\rangle/\sqrt{l!}$ are constructed out of the PS with the help of the raising operator \hat{k}_- [7]. Any PS carries the exact quantum number $k = 0$ (while a daughter state in the l -th generation carries $k = l$). The additional requirement of conservation of k for allowed electric-dipole transitions means that *parent states*, $|\Psi_{M_z}^{(P_i)}\rangle$ and $|\Psi_{M_z'}^{(P_j)}\rangle$ in the two families, must satisfy $M_z' = M_z \pm 1$ for there to be allowed FIR transitions. The PS's in the (00) and (10) LL's have $M_z = -1$ and $M_z' = +1$, and do not satisfy this requirement. Therefore, the family of X_{t10}^- bound states is *dark*, i.e., is not accessible by internal transitions from the ground X_{t00}^- bound states. Breaking of translational invariance (by impurities, disorder etc.) would make the $X_{t00}^- \rightarrow X_{t10}^-$ transition allowed.

Most qualitative features discussed above are preserved at finite fields and confinement where both triplet and singlet bound X^- states exist, as shown by calculations for a representative case (200 Å GaAs/Ga_{0.7}Al_{0.3}As QW at $B > 9$ T). We obtain eigenstates of X^- using an expansion [12,9] in e and h LL's and size-quantization levels in a QW; we assume a simple valence band for holes with in-plane $m_{h\parallel} = 0.24$ and perpendicular $m_{hz} = 0.34$ effective masses ($m_e = 0.067$ is isotropic, the GaAs dielectric constant $\epsilon = 12.5$). For the singlet and triplet binding energies of X^- in the zeroth LL we obtain results equivalent to the high-accuracy calculations of [9]. Both singlet and triplet transitions exhibit a characteristic double-peak structure, but the singlet transitions are broader, and the peak at higher energies has a larger oscillator strength. Results for the singlet transitions at 9 Tesla are shown in Fig. 2(a). For comparison with the theoretical calculations we have studied two 20 nm wide GaAs/Al_{0.3}Ga_{0.7}As multi-

ple quantum well (MQW) structures, one undoped and one modulation-doped in the barrier with silicon donors at $2 \times 10^{10} \text{ cm}^{-2}$, by optically detected resonance (ODR) spectroscopy [15]. Both samples show the X^- -photoluminescence (PL) line. The experiment confirms the theoretical predictions discussed above. In Fig. 2(b) a series of ODR scans for the undoped sample is shown at several FIR laser wavelengths. During the magnetic field sweep the spectrometer was stepped to remain centered on the peak of the X^- -recombination line. The recorded changes in the PL intensity (ΔI_{PL}) of the X^- -PL line correspond to a decrease in the PL intensity of X^- . Tracking the PL peak of X instead of X^- yields ODR scans which are inverted (increase in PL strength), but otherwise very similar. The spectra in Fig. 2(b) are displaced in magnetic field such as to align the position of the sharp, negative going electron cyclotron resonance (e-CR) present in all scans at the position of the e-CR at $118.8 \mu\text{m}$, 6.23 Tesla. In this way, the behavior of features occurring at lower magnetic fields, and with an amplitude approximately one order of magnitude smaller than e-CR, are more easily seen.

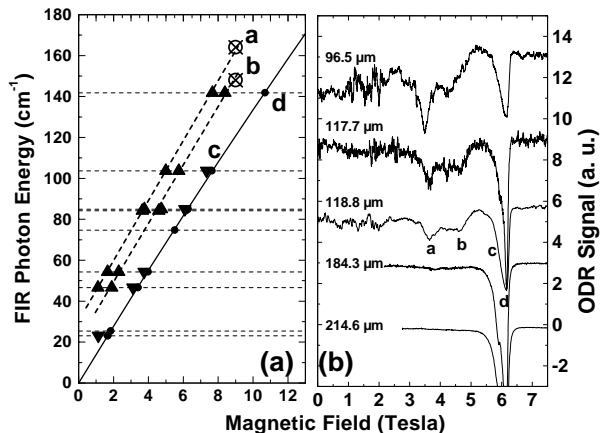


FIG. 2. (a) Summary plot of the observed internal transitions of X^- as a function of magnetic field. Dashed lines are guides to the eye, the solid line represents a fit through the measured positions of electron cyclotron resonance. The crossed out circles at 9 T are the results of the calculation described in the text. (b) ODR scans as a function of magnetic field for several FIR laser wavelengths. The horizontal (B) scale corresponds to the scan taken at $118.8 \mu\text{m}$. (a) and (b) denote the X^- -singlet transitions and (c) marks the X^- -triplet transition.

These ODR scans show several resonances at magnetic fields below that of e-CR. For instance, the

ODR scan recorded at a FIR wavelength of $118.8\ \mu\text{m}$ has features at 4.08 Tesla (a) and 4.60 Tesla (b), in addition to a shoulder roughly 0.1 Tesla (c) below e-CR (d). Resonances of similar shape are observed in all ODR scans recorded with FIR wavelengths shorter than $393.6\ \mu\text{m}$. At $393.6\ \mu\text{m}$ and $432.6\ \mu\text{m}$ no resonances were observed at magnetic fields below e-CR. The qualitative behavior of the modulation-doped sample is very similar; however, the strength of features (a) and (c) at lower magnetic fields is greatly enhanced with respect to e-CR. In this sample the intensity of the X^- -PL line is much larger than in the undoped structure, so X^- -features are expected to be stronger.

The observed resonances are summarized in Fig. 2(a), where the peak positions in the ODR scans for the undoped sample are plotted as a function of magnetic field for all measured FIR laser lines. Features labeled (a) and (b) in Fig. 2(b) are shown by upright triangles, feature (c) is represented by an inverted triangle, and e-CR is marked by solid circles. Features (a) and (c) occur in the modulation-doped sample approximately 0.1 Tesla lower than the data points in this figure. Feature (b) is observed at elevated temperature. Two points from the numerical calculation for the singlet transitions at 9 Tesla are plotted as crossed-out circles at the end of the two dashed lines, which are guides to the eye. The predicted double-peak structure for the X^- -singlet transition is clearly observed and in good agreement with the calculations.

Based on the discussion above and the good qualitative as well as quantitative agreement of the experiment with theory, we assign features (a) and (b) to the internal X^- -singlet transition, and feature (c) to the internal X^- -triplet transition. No evidence was found for any features on the high-field size of e-CR corresponding to the localized-to-localized state transitions (*e.g.* the X^- -triplet) that are dominant in magneto-spectroscopy of D^- . In conclusion, photoionizing spin-singlet and spin-triplet transitions of X^- have been observed experimentally. The experimental findings are in good agreement with theoretical predictions, which show that due to an additional exact selection rule resulting from a hidden symmetry, the bound-to-bound X^- singlet- and triplet-transitions to the next electron LL are forbidden. The appearance of a corresponding triplet fea-

ture *below* the e-CR energy should be a characteristic feature associated with breaking of translational invariance. This may be used as a tool for studying the extent of X^- localization.

ABD is grateful to the Department of Physics, University at Buffalo, where part of this work was performed, and to the Humboldt Stiftung for financial support. The work at SUNY at Buffalo was supported by NSF grant DMR 9722625.

-
- * on leave from General Physics Institute, RAS, Moscow 117942, Russia.
- [1] K. Kheng, R.T. Cox, Merle Y. d'Aubigné *et al.* Phys. Rev. Lett. **71**, 1752 (1993).
 - [2] Z.X. Jiang, B.D. McCombe, J.-L. Zhu *et al.*, Phys. Rev. B **56**, R1692 (1997), and references therein.
 - [3] W. Kohn, Phys. Rev. **123**, 1242 (1961).
 - [4] I.V. Lerner and Yu.E. Lozovik, Sov. Phys. JETP **51**, 588 (1980).
 - [5] A.B. Dzyubenko, Phys. Lett. A **165**, 357 (1992); **173**, 311 (1993).
 - [6] J.E. Avron, I.W. Herbst, and B. Simon, Annals of Phys. **114**, 431 (1978).
 - [7] A.B. Dzyubenko and A.Yu. Sivachenko, cond-mat/9902086.
 - [8] J.J. Palacios, D. Yoshioka, and A.H. MacDonald, Phys. Rev. B **54**, R2296 (1996).
 - [9] D.M. Whittaker and A.J. Shields, Phys. Rev. B **56**, 15 185 (1997).
 - [10] J. Cerne, J. Kono, M.S. Sherwin *et al.* Phys. Rev. Lett. **77**, 1131 (1996); M. Salib, H.A. Nickel, G.S. Herold *et al.* Phys. Rev. Lett. **77**, 1135 (1996).
 - [11] A.B. Dzyubenko, Pis'ma ZhETF, **66**, 588 (1997) [JETP Lett. **66**, 617 (1997)].
 - [12] A.B. Dzyubenko and A.Yu. Sivachenko, Phys. Rev. B **48**, 14 690 (1993).
 - [13] R.S. Ryu, Z.X. Jiang, W.J. Li *et al.* Phys. Rev. B **54**, R11 086 (1996).
 - [14] The Hamiltonian of the interaction with the FIR radiation of polarization σ^\pm is of the form $\hat{V}^\pm \sim \sum_j e_j \pi_j^\pm / m_j$, where $\pi_j^\pm = \pi_{jx} \pm i\pi_{jy}$, and commutes with $\hat{\mathbf{K}}$ (and $\hat{\mathbf{K}}^2$).
 - [15] see *e.g.*: H.A. Nickel, G.S. Herold, M.S. Salib *et al.*, Physica B **249-251**, 598 (1998), and references therein.